

Nuclear antiferromagnetic ordering of the Van Vleck paramagnet PrIn_3

Yoshitomo Karaki, Minoru Kubota, and Hidehiko Ishimoto

Institute for Solid State Physics, University of Tokyo, Roppongi, Minato-Ku, Tokyo 106-8666, Japan

Yoshichika Ōnuki

Department of Physics, Osaka University, Toyonaka, Osaka 560-0043, Japan

(Received 25 November 1998)

Magnetization and ac susceptibility measurements have been performed on the intermetallic compound PrIn_3 down to temperatures well below the ordering temperature 0.14 mK, the lowest among Van Vleck paramagnets. No divergence of susceptibility or spontaneous magnetization was observed which would indicate the antiferromagnetic transition. The obtained Weiss temperature is negative and extremely small, -0.01 mK. A possible antiferromagnetic spin structure is discussed within a mean field approximation.

[S0163-1829(99)13333-2]

Nuclear magnetic ordering is expected to appear at millikelvin temperatures or below because of nuclear magnetic moments which are three orders of magnitude smaller than electronic moments. There are two exceptions to this: bcc solid He^3 and Van Vleck paramagnets. For bcc solid He^3 the exchange interaction between neighboring spins is produced by a large zero point motion, causing the ordering phenomenon in the millikelvin temperature range. The nuclear magnetic ordering of Van Vleck paramagnets occurs with the help of the electronic moment at millikelvin and submillikelvin transition temperatures. The Korringa constants in such metallic compounds as Pr alloys are considerably smaller than those of pure metals, e.g., Cu or Ag because of strong coupling of Pr nuclei with the conduction electron. Therefore, the nuclear spin temperature is always equal to the conduction electron temperature which can be measured by a conventional platinum NMR thermometer. Thermodynamic study on nuclear magnetic ordering of metallic Van Vleck paramagnets can be carried out more easily than pure metals in which temperature determination in the ordered state is problematic.

Owing to large Van Vleck susceptibility and hyperfine interaction of Pr compound, the nuclear moment is enhanced by a factor of $1 + K$, typically 8–20, from the bare value.¹ A larger reduction of the nuclear spin entropy is thus easily obtained at rather high temperatures and moderate external fields in comparison to pure Cu or Ag. Consequently, Pr intermetallic compounds with a low magnetic ordering temperature have often been studied as coolants for nuclear demagnetization: Ferromagnetic ordering has been observed for PrCu_6 ($T_C = 1.7$ mK) (Refs. 2 and 3) and PrNi_5 ($T_C = 0.4$ mK).⁴ Nonferromagnetic susceptibility anomaly was found for PrSe below 1 mK.⁵ Antiferromagnetic ordering was observed for PrBe_{13} ($T_N = 0.4$ mK) (Ref. 6) and PrIn_3 ($T_N = 0.14$ mK).⁷ In the theoretical point of view, Nagashima and Ishii recently pointed out the importance of orbital degeneracy of the $4f$ electron in their calculation of the s - f interaction in a singlet ground state on Pr intermetallic compounds and obtained a new type of Ruderman-Kittel-Kasuya-Yosida (RKKY) interaction between Pr nuclear spins with a form $I_i \hat{J}(\mathbf{R}_{ij}) I_j$, where the elements of the tensor $\hat{J}(\mathbf{R}_{ij})$ depend not only on R_{ij} but also on the angle of

\mathbf{R}_{ij} relative to the crystal axis.⁸ They predicted a possible nuclear spin structure due to the RKKY interaction in the mean field approximation: For the antiferromagnetic ordering, a sinusoidal or a helical structure was predicted near T_N . In the former case, another first order transition to a helical one is expected at a temperature between T_N and $T = 0$. This makes it of interest to study the case of antiferromagnetic ordering experimentally.

Here we report experimental results on PrIn_3 which has a relatively small enhancement factor $1 + K = 6.7$ (Ref. 9) and hence a low magnetic ordering temperature. The crystal structure is a simple cubic AuCu_3 type. However, the lowest temperature achieved by nuclear demagnetization cooling of the sample itself was limited by the existence of large nuclear quadrupole interaction of indium as suggested by Asahi *et al.*¹⁰ Our previous specific heat measurement on single crystal PrIn_3 down to 0.07 mK (Ref. 7) revealed (Fig. 1) that the nuclear quadrupole interaction of indium has a positive sign of $\nu_q = +228$ MHz, where ν_q is defined as $h\nu_q = e^2 q Q$ and Q denotes the nuclear quadrupole moment of indium. The sharp specific heat anomaly observed at 0.14 mK proves the existence of nuclear magnetic ordering. Nev-

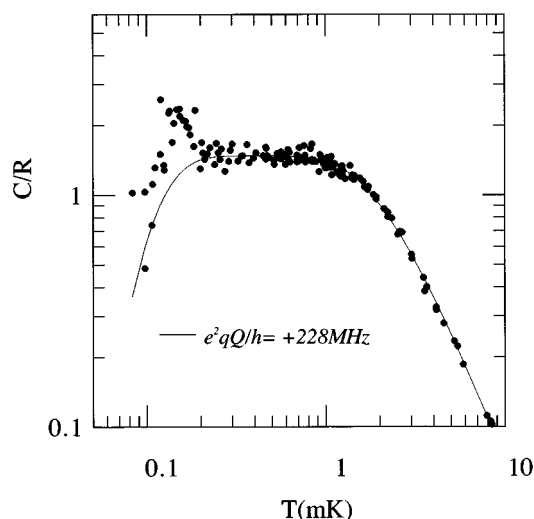


FIG. 1. Specific heat of PrIn_3 . Based on Fig. 1 in Ref. 1 with new data added. The line shows the calculated specific heat for Indium nuclear quadrupole interaction of $\nu_q = +228$ MHz.

ertheless the character of magnetic ordering is not yet clear, and measurement of the magnetization across the transition temperatures is essential.

The experiment was performed using the same double stage nuclear demagnetization cryostat as used for the specific heat measurement.⁷ The first stage was 24 moles of Cu. The second stage coolant was 0.0451 mole (21.9 g) of PrIn_3 and the sample was mounted on this stage. These two stages were connected by a tin superconducting heat switch. The first stage, precooled by a dilution refrigerator to about 11 mK in 9 T field, usually cools the second stage down to about 0.2 mK in 0.6 T field. The temperatures of both stages were measured by two platinum NMR thermometers below 20 mK; above 20 mK, resistance thermometers were employed. Thermometers were calibrated against a ^3He melting curve thermometer attached to the first stage. The lowest temperature observed after the demagnetization of the second stage to zero field was about 50 μK .

Single crystal rods of PrIn_3 were grown by the Czochralski pulling method.¹¹ It was cut into a slab ($0.2 \times 2.0 \times 10 \text{ mm}^3$) with a wire spark cutter. The amount of the sample was 6.2×10^{-5} mole (30 mg) and the residual resistivity was $0.16 \mu\Omega \text{ cm}$, corresponding to the residual resistivity ratio of 160. The surface was polished with No. 2000 emery paper. The lower half of the sample was sandwiched by a high purity silver sample holder and glued with a conducting epoxy.¹² The sample holder was attached to the second demagnetization stage with three silver screws 3 mm in diameter. The thermal conductance between the sample and the thermometer was estimated by the Wiedemann-Franz law to be $2 \times 10^{-3} T (\text{W/K})$ from the corresponding electrical resistance $R = 12 \mu\Omega$ and the Lorenz number $L_0 = 2.45 \times 10^{-8} \text{ W } \Omega / \text{K}^2$. Then, the heat flow \dot{Q}_s from the sample to the second stage was calculated, assuming a negligible direct heat leak to the sample and the same temperature rise of the sample and the second stage. The observed temperature rise of $dT/dt = 1.3 \times 10^{-10} \text{ K/sec}$ and the sample heat capacity of $1.5 \times 10^{-3} \text{ J/K}$ at $T_N (0.14 \text{ mK})$ led to \dot{Q}_s of $2.0 \times 10^{-13} \text{ W}$ and therefore a negligible temperature difference of 0.7 μK between the sample and the thermometer.

Magnetization and ac susceptibility were measured using a SHE RLM measuring system where a SQUID was employed as a null detector. A superconducting astatic pair of secondary coils and a primary coil were wound on a quartz tube 8 mm in outer diameter and 1 mm in thickness. The coil system was put inside a tantalum tube which was used to trap a stable magnetic field. The tube was installed in a small superconducting solenoid with a niobium tube outside and with a heater and a resistance thermometer on the body. The whole system was supported mechanically on the second nuclear stage by four Vespel SP-22 rods (4 mm in diameter) and thermally anchored to the mixing chamber of the dilution refrigerator. The dc and ac magnetic fields were applied almost parallel to (111) direction of the PrIn_3 single crystal. An ac excitation magnetic field was 4 μT peak to peak with a frequency of 16 Hz. To trap a static magnetic field, the entire system was once heated to a temperature higher than the superconducting transition temperature of tantalum ($T_C = 4.38 \text{ K}$ at zero field) and lower than T_C of the niobium shield and Nb-Ti wire of the solenoid. The heater was then

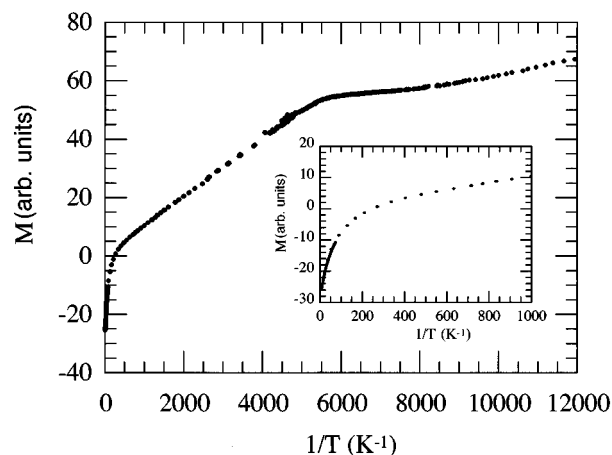


FIG. 2. Magnetization as a function of inverse temperature at 3 mT field. The inset shows the high-temperature portion of the data.

turned off and the tantalum tube cooled across the superconducting transition under an applied field. Because of rather weak thermal coupling between the mixing chamber and the coil system, the mixing chamber temperature did not rise above 200 mK for a while even though the tantalum tube was heated to around 5 K. The trapped fields were 1, 3, and 30 mT.

Figure 2 shows the magnetization as a function of inverse temperature in 3 mT field. The vertical axis corresponds to the output voltage of the SQUID magnetometer and therefore to the change of magnetization. The jump of the output voltage caused by resetting the SQUID was connected smoothly on a chart recorder. The change of slope around 5 mK was due to saturation of the magnetization arising from paramagnetic impurities under the applied magnetic field, since the starting material Pr of our sample contained 10 ppm of Fe and 3 ppm of Mn impurities. ac susceptibilities at 1, 3, and 30 mT are shown in Fig. 3. The broad peak around 10 mK at 3 mT also shows the beginning of the saturation. To discuss nuclear magnetization, we use the data in the lower-temperature region where the impurity magnetization is saturated.

The low-temperature part of the magnetization and ac susceptibility at 3 mT is shown in Fig. 4 as a function of temperature in addition to the specific heat of Pr nuclear spin. Divergence of susceptibility was not observed at the ordering temperature of $T_N = 0.14 \text{ mK}$. Furthermore, spontaneous magnetization did not exist because the magnetization and ac susceptibility showed the same temperature dependence. This fact indicates that the nuclear magnetic ordering of PrIn_3 was antiferromagnetic. There was no first order transition below T_N , which is expected for the sinusoidal spin ordering at T_N as proposed by Nagashima and Ishii in the measured temperature range. No decrease on the observed susceptibility below the ordering temperature suggests that it is a perpendicular susceptibility, although the reason for the increase of magnetization below T_N is not clear. One possible explanation is spin wave excitation.¹³ The perpendicular susceptibility may not necessarily mean that an easy axis is perpendicular to the applied field. If a spin-flop transition exists below the lowest applied field 1 mT, the easy axis is parallel to the applied field.

The measured magnetization consists of Pr and indium

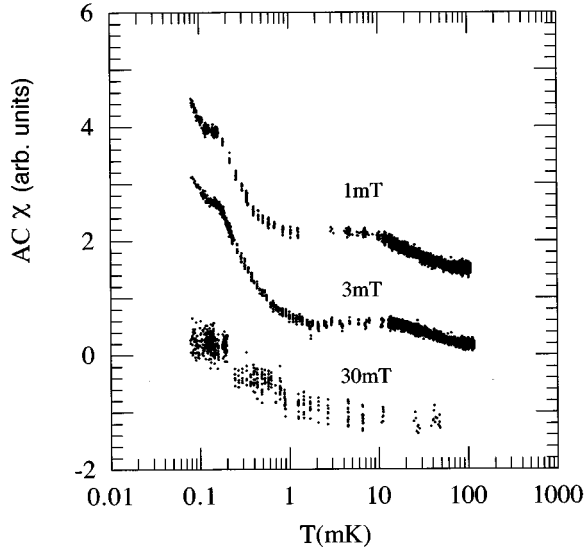


FIG. 3. Temperature dependence of ac susceptibilities at 1, 3, and 30 mT. The vertical axis is shifted for each magnetic field.

magnetization. Although the latter is about ten times smaller than the former, indium magnetization must be subtracted to accurately determine the Weiss temperature of Pr nuclear spin. The magnetization of indium nuclei can be calculated, assuming the spin-spin interaction is negligible. The spin Hamiltonian of indium is given by

$$H = DI_z^2 - g_{In}\mu_N I_z B (I=9/2), \quad (1)$$

where D is defined as $D = 3h\nu_q/4I(2I-1)$, g_{In} is the g factor of indium nuclear spin, and μ_N is the nuclear magneton. The z axis is parallel to the symmetry axis of the electric field gradient eq and the z' axis is parallel to the applied field B . Three indium atoms in a unit cell have three orthogonal symmetry axes of the electric field gradient. Indium on the (100) plane has the symmetry axis parallel to the [100] axis. The other two indiums on (010), (001) planes have the symmetry axes parallel to [010] and [001], respectively. Since the external magnetic field was applied in parallel to [111],

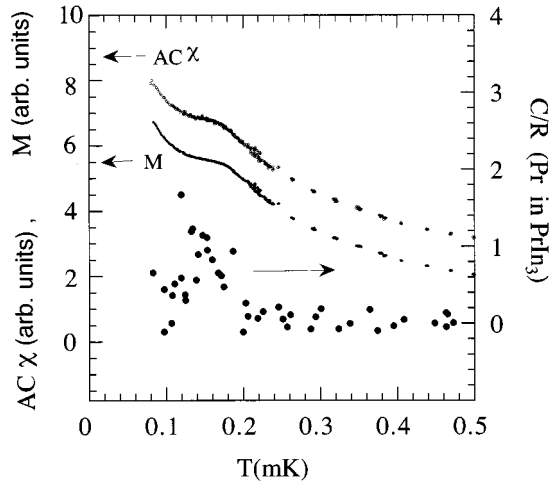


FIG. 4. Low-temperature part of magnetization and ac susceptibility at 3 mT. The specific heat of Pr nuclear spin is also shown after subtracting the indium nuclear quadrupole interaction ($\nu_q = +228$ MHz) from the measured specific heat.

TABLE I. Results of fitting parameters. C_{In} and T_D are obtained by fitting the numerical calculation of indium magnetization to Eq. (2). η and Θ are obtained by fitting the experimental data to Eqs. (3) and (4).

	C_{In} (emu/mole)	T_D (μ K)	η	Θ (μ K)
1 mT	4.682×10^{-7}	+41.7	7.640	+1.4
3 mT	4.702×10^{-7}	+41.9	7.488	+9.5
30 mT	4.731×10^{-7}	+45.6	7.323	+41.3

the angles θ between the symmetry axes of the electric field gradient and the external magnetic field are identical for the three sites, $\cos \theta = 1/\sqrt{3}$. Indium at each site thus has the same magnetization, which is calculated from numerical diagonalization of Eq. (1) and is expressed as a simple empirical formula

$$M_{In} = BC_{In}/(T + T_D). \quad (2)$$

Here, C_{In} is the Curie constant per 1 mole of Indium nuclear spins and T_D is a constant which depends on D . Both are determined by fitting the calculated results of magnetization to Eq. (2). The magnetization of Pr nuclei can be expressed in the paramagnetic state as

$$M_{Pr} = BC_{Pr}/(T - \Theta), \quad (3)$$

$$C_{Pr} = N_A (g_{Pr}\mu_N)^2 (1 + K)^2 I(I+1) / 3k_B,$$

where C_{Pr} is a Curie constant per 1 mole of Pr nuclear spins, $N_A = 6.02 \times 10^{23}$ is the Avogadro number, $g_{Pr} = 1.71$ is the g factor of Pr nuclear spin, and Θ is the Weiss temperature. The total magnetization M and the output voltage of the SQUID magnetometer V_{sq} are written as

$$M = 3M_{In} + M_{Pr}, \quad V_{sq} - V_0 = \eta M, \quad (4)$$

where V_0 is the output voltage of the SQUID magnetometer for the infinite nuclear spin temperature. η is a parameter which depends on the sensitivity of the SQUID, the pick up coil geometry, the dimensions, and density of the sample. The obtained magnetization data are fitted to Eq. (4) using three fitting parameters V_0 , η and Θ . The obtained values η , Θ and C_{In} , T_D from those fittings are listed in Table I. Scattering of η at different fields is within 2%, which confirms the reliability of the measuring system and the analysis. The absolute value of magnetization can be discussed using the obtained value of η . The ratio M/M_S of Pr nuclear spin is only 0.028 at T_N and at 3 mT, where M_S is the saturation magnetization given by $M_S = N_A g_{Pr}\mu_N (1 + K)I$. This small value of M/M_S also assures there is no ferromagnetic nature of the ordering.

The temperature dependence of susceptibilities (M/B) of Pr nuclear spin at 1, 3, and 30 mT is shown in Fig. 5. The solid lines represent the Curie-Weiss fitting with the obtained η and Θ in each field. Temperature dependence of the inverse susceptibilities is shown in the inset, where the solid lines also correspond to the Curie-Weiss fitting. The Weiss constant $\Theta = -0.01 \pm 0.01$ mK is determined by the results at 1 and 3 mT, since the Zeeman splitting of Pr nuclear spin at $B = 30$ mT is comparable to the ordering temperature, that is, the nuclear spin-spin interaction.

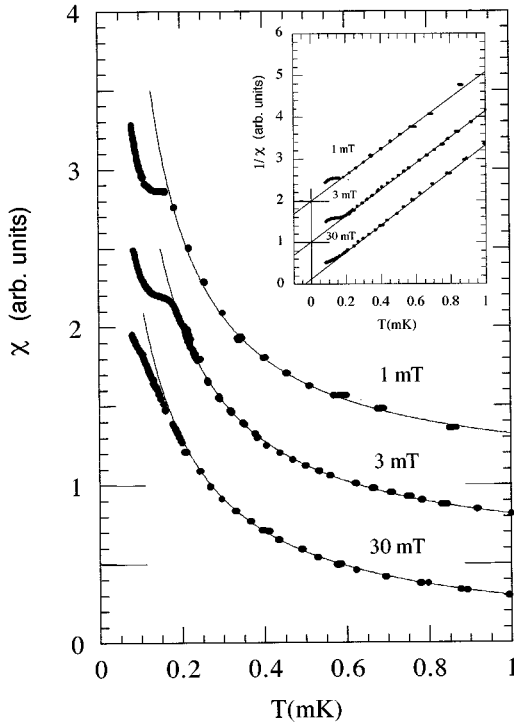


FIG. 5. Susceptibilities (M/B) of Pr nuclear spin versus temperature in magnetic fields of 1, 3, and 30 mT. The vertical axis for 1 and 3 mT is shifted by 1.0 and 0.5, respectively. The solid lines show the Curie-Weiss fitting as described in the text. Inset shows inverse susceptibilities $(M/B)^{-1}$ of Pr nuclear spin as a function of temperature at 1, 3, and 30 mT. The vertical axis for 1 and 3 mT is shifted 2.0 and 1.0, respectively.

To apply a simple mean field approximation¹⁴ to the effective Hamiltonian,¹⁵ we assume two different effective exchange constants, J_1 and J_2 , J_1 being the nearest neighbor effective exchange constant and J_2 being the next nearest. The effective spin Hamiltonian is written as

$$H = -2J_1 \sum_{\langle ij \rangle 1} I_i I_j - 2J_2 \sum_{\langle ij \rangle 2} I_i I_j, \quad (5)$$

where $\langle ij \rangle 1$ and $\langle ij \rangle 2$ mean pairs of nearest neighbor spins and next nearest ones, respectively. Two solutions, type I AF

and type III AF for the simple cubic lattice, are obtained for $T_N = 0.14$ mK and $\Theta = -0.01$ mK. For the type I structure, the mean field equations are given by

$$T_N = (-12J_1 + 24J_2)I(I+1)/3k_B, \\ \Theta = -(-12J_1 - 24J_2)I(I+1)/3k_B. \quad (6)$$

The solution is $J_1/k_B = -2.1 \mu\text{K}$ and $J_2/k_B = 0.93 \mu\text{K}$. The type I structure is a simple spin one, where nearest neighbor spins are aligned anti-parallel and next nearest neighbors are aligned parallel. For type III, the equations are

$$T_N = (4J_1 - 8J_2)I(I+1)/3k_B, \\ \Theta = -(-12J_1 - 24J_2)I(I+1)/3k_B. \quad (7)$$

The solution is $J_1/k_B = 5.9 \mu\text{K}$ and $J_2/k_B = -3.1 \mu\text{K}$. The type III structure has ferromagnetic planes [for example, (001)] whose spin direction varies alternatively. The critical magnetic fields for both cases are given as $B_C = -24J_1 \langle I \rangle \{g_{\text{Pr}} \mu_N (1+K)\}$ for type I and $B_C = (-8J_1 - 32J_2) \langle I \rangle \{g_{\text{Pr}} \mu_N (1+K)\}$ for type III. The calculated values for the two spin structures are almost equal, $B_C = 31$ mT ($T=0$), and it is difficult to determine the realized spin structure from the magnetization process. The above discussion based on two exchange parameters is not satisfactory because the long-range nature of the RKKY interaction is not taken into account. However, the extremely small value of $|\Theta|/T_N = 0.08$ means that the nearest neighbor interaction is almost canceled by the next nearest or further distant neighbor interactions.

In summary, we observed the nuclear antiferromagnetic ordering of Van Vleck paramagnet PrIn_3 with magnetization and ac susceptibility measurements. The first order transition expected for the sinusoidal spin ordering below T_N was not observed within the range of the present measurements. We propose two possible spin structures from the mean field calculation using the ordering temperature $T_N = 0.14$ mK and the Weiss temperature $\Theta = -0.01$ mK.

The authors would like to thank Y. Koike for his help during the experiments. They are grateful to H. Ishii and T. Nagashima for valuable discussions. Y.K. was supported by Grant-in-Aid for Scientific Research (C) from the Ministry of Education, Science and Culture of Japan.

¹K. Andres, *Cryogenics* **18**, 473 (1978).

²J. Babcock, J. Kiely, T. Manley, and W. Weyhmann, *Phys. Rev. Lett.* **43**, 380 (1979).

³T. Fukuda, H. Ishimoto, H. Fukuyama, S. Ogawa, Y. Ōnuki, and T. Komatsubara, *J. Phys. Soc. Jpn.* **59**, 2496 (1989).

⁴M. Kubota, H. R. Folle, Ch. Buchal, R. M. Mueller, and F. Po-bell, *Phys. Rev. Lett.* **45**, 1812 (1980).

⁵M. Kubota, K. J. Fischer, and R. Mueller, *Jpn. J. Appl. Phys., Suppl.* **26-3**, 427 (1987).

⁶P. L. Moyland, T. Lang, E. D. Adams, G. R. Stewart, and Y. Takano, *Czech. J. Phys.* **46**, 2199 (1996).

⁷Y. Karaki, Y. Koike, M. Kubota, H. Ishimoto, and Y. Ōnuki, *Czech. J. Phys.* **46**, 2209 (1996).

⁸N. Nagashima and H. Ishii, *J. Phys. Soc. Jpn.* **67**, 1431 (1998).

⁹K. Satoh, Y. Kitaoka, H. Yasuoka, S. Takayanagi, and T. Sugawara, *J. Phys. Soc. Jpn.* **50**, 351 (1981).

¹⁰K. Asahi, N. Nishida, S. Kobayashi, J. Ray, A. Nakaizumi, Y. Iseki, K. Terui, T. Sugawara, H. Ishimoto, and K. Ono, *Phys. Lett.* **82A**, 244 (1981).

¹¹I. Umehara, N. Nagai, and Y. Ōnuki, *J. Phys. Soc. Jpn.* **60**, 3150 (1991).

¹²Eccobond 83C and catalyst 9; GRACE JAPAN Co., Ltd.

¹³R. Kubo, *Phys. Rev.* **87**, 568 (1952); J. Kanamori and K. Yoshida, *Prog. Theor. Phys.* **14**, 423 (1955).

¹⁴D. ter Haar and M. E. Lines, *Philos. Trans. R. Soc. London, Ser. A* **245**, 1046 (1962).

¹⁵T. Murao, *J. Phys. Soc. Jpn.* **39**, 50 (1975).